Automatika

Journal for Control, Measurement, Electronics, Computing and Communications

ISSN: 0005-1144 (Print) 1848-3380 (Online) Journal homepage: https://www.tandfonline.com/loi/taut20

Improvement of control precision for ship movement using a multidimensional controller

Monika Rybczak

To cite this article: Monika Rybczak (2018) Improvement of control precision for ship movement using a multidimensional controller, Automatika, 59:1, 63-70, DOI: 10.1080/00051144.2018.1499427

To link to this article: https://doi.org/10.1080/00051144.2018.1499427

© 2018 The Author(s). Published by Informa UK Limited, trading as Taylor & Francis Group

Published online: 23 Jul 2018.

Submit your article to this journal

Article views: 196

View related articles

View Crossmark data

Full Terms & Conditions of access and use can be found at
https://www.tandfonline.com/action/journalInformation?journalCode=taut20

AUTOMATIKA
2018, VOL. 59, NO. 1, 63–70
https://doi.org/10.1080/00051144.2018.1499427

REGULAR PAPER

OPEN ACCESS Check for updates

Improvement of control precision for ship movement using a multidimensional controller

Monika Rybczak

Department of Ship Automation, Gdynia Maritime University, Gdynia, Poland

ABSTRACT
This paper presents the influence of a first stage inertial element on the operation of a state space controller for a third dimension object. First chapter presents a brief introduction to linear matrix inequalities as one of the methods of controller analysis and synthesis, with examples, and helps to places the below paper in this wide field of science. Chapter two presents the controlled object, which is a model of a very large crude carrier (VLCC) ship, called *Blue Lady*, along with its mathematical state space model. Chapter three shows state space controller design using numerical methods of linear equalities optimization, where the given values are *u* longitudinal, *v* lateral and *r* rotational velocities. Presented there is also the implementation method of an inertial element to a multidimensional object for space state controller synthesis. Chapter four shows computer simulation results and focuses on showing influence of the proposed design on control error of the multidimensional closed loop system. Finally, chapter five concludes and comments simulation results and shows possible direction of future studies.

ARTICLE HISTORY
Received 14 June 2017
Accepted 6 July 2018

KEYWORDS
Linear matrix inequalities; inertial element; integrating element; multidimensional ship control; state space control; use LMI

1. Introduction

Within the last several years many new tools have been created for controller analysis and synthesis that allow solving complex control problems. Among them are systems with analytical uncertainty estimation and some classes of non-linear systems which utilize optimization algorithms [1–5]. A possible solution to the problem can be synthesizing a control system that assures minimum or maximum of a target function with its restrictions or confirming that no viable solution exists. Also the problem of multidimensional control, which means controlling more than two output values, has to be considered [6–8]. As the above methods grew more popular so did numerical methods to solve them, such as linear matrix inequalities (LMI), a method used in analysis and synthesis of control systems. These are described in detail in [9,10]. In [11], the authors show LMI use in multidimensional systems with a *Fuzzy Logic Controller*. While in [12] the authors go back to formulating different LMI problems using s-functions. While the authors of [13,14] claim that it is always possible to find a solution, with an acceptable precision, using high performance LMI algorithms. Controller synthesis using LMI leads to effective numerical solutions, backed up by promising computer simulation results as shown in [13] where the chapter about applications of a closed loop system shows results of computer simulations, where the space state controller for a missile, controls its flight path. It is estimated that several dozen new publications about the use of LMI are written each year, for example, in 2017 a total of 41 were registered in IEEE database. However, majority of them describe the use of LMI in land-based applications and only seldom in marine applications. Examples of the very few marine applications include papers [15–17] where the authors compare an LMI controller designed using H_∞ with a robust controller for a multidimensional ship model. Also paper [18] shows a stabilized platform with two degrees of freedom (2DOF) used for stabilizing equipment like satellite antennas or cameras on board ships. First controller synthesis using H_2 and H_∞ standards and pole placement restrictions for output interference compensation is presented. Later experimental results are presented of when the platform with a satellite antenna was installed on board a ship and tested by tracking satellite signal at different sea conditions. The author being closely related to marine automation and marine industry decided to focus her work on this area of LMI use. This paper presents a controller for precise ship movement control, among others at low speeds, similar to dynamic positioning systems. Inertial element proposed in this paper is used to reduce control error to the multidimensional control system.

CONTACT Monika Rybczak m.rybczak@we.am.gdynia.pl, rybczak.monika@gmail.com, rybczak.monika@gmail.com Department of Ship Automation, Gdynia Maritime University, ul. Morska 83, Gdynia 81-225, Poland

© 2018 The Author(s). Published by Informa UK Limited, trading as Taylor & Francis Group.
This is an Open Access article distributed under the terms of the Creative Commons Attribution License (http://creativecommons.org/licenses/by/4.0/), which permits unrestricted use, distribution, and reproduction in any medium, provided the original work is properly cited.

2. Multidimensional object

2.1. Training ship

State space controller synthesis using LMI was done for a multidimensional model which was a ship model of a very large crude carrier (VLCC) ship called *Blue Lady* as shown in Figure 1. The model is isomorphous to a real VLCC ship, built with retention of geometric, kinematic and dynamic similarity laws. The *Blue Lady* ship model is built in 1:24 scale to a real VLCC ship, used for transportation of crude oil. Basic dimensions of the model are length 13.75 m, breadth 2.38 m, maximum speed 1.59 m/s to 3.1 kn.

The simulation model is based on papers of W. Gierusz as shown in [19,20]. It belong to 3DOF class, and takes into account movement on a single plane without including list, trim and draught during Silm Lake trials as described in [21,22].

2.2. Mathematical state space model

The controlled object is a multidimensional, non-linear real life object. When modelling ships dynamics for the use of controller synthesis, model linearization around the working point was used [23]. Object identification process included thruster operation, ship's hull construction, set of stationary Kalman filters (used for recreation of u, v and r velocities), power distribution system used for calculating three components of **u** velocity vector:

$$\mathbf{u} = [\tau_x, \tau_y, \tau_r]^{\mathrm{T}} \tag{1}$$

The controlled object takes into account three input signals: τ_x, τ_y, τ_r and three output signals: $\hat{u}, \hat{v}, \hat{r}$, where τ_x – required force (thrust) on the ships longitudinal axis, τ_y – required force (thrust) on the ships lateral axis, τ_r – required rotational force. Given signals are considered as components of input signal vectors to blocks in which forces and moments are calculated. Command signals are ng_c – main propeller rotation speed, σ_c – rudder blade angle, $sstd_c$ – relative thrust of the forward tunnel thruster, $sstr_c$ - relative thrust of the aft tunnel thruster, $ssod_c$ – relative thrust of the forward rotational tunnel thruster, α_{dc} – rotation angle of the forward

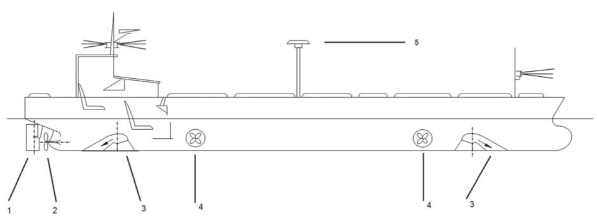

Figure 1. *Blue Lady* ship model silhouette. The model is equipped with a two-person control station used for controlling all of ship operations. 1, rudder blade; 2, main propeller; 3, rotational tunnel thrusters; 4, tunnel thrusters; 5, DGPS antenna.

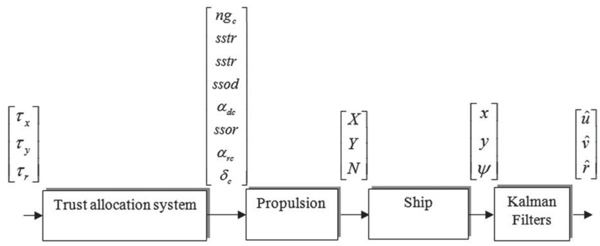

Figure 2. Block diagram of the controlled system for identification process u, v, r – ships velocities, x, y, ψ – ships position and course, $[ng_c, sstd_c \ldots]^{\mathrm{T}}$ vectors – command signals for propulsion and steering equipment, $[X_l Y_l N_l]^{\mathrm{T}}$ vectors – forces and moments generated by propulsion and steering equipment, $\hat{u}, \hat{v}, \hat{r}$.

rotational tunnel thruster, $ssor_c$ – relative thrust of the aft rotational tunnel thruster, α_{rc} – rotation angle of the aft rotational tunnel thruster. The above signals are connected to a block that is responsible for modelling dynamics of all ship's propulsion and control elements. These are the main propeller, rudder blade, forward and aft tunnel thrusters and forward and aft rotational tunnel thrusters. Figure 2 shows a block diagram of the controlled object with all signals of the *Blue Lady* ship model.

As a result of the identification process numerical values were calculated for the *Blue Lady* ship model coefficients that were later used in Equations (2) . The presented state space model is a nominal (average) model and its state space equations and output equations are as follows:

$$\begin{bmatrix} \dot{x}_1 \\ \dot{x}_2 \\ \dot{x}_3 \end{bmatrix} = A \begin{bmatrix} x_1 \\ x_2 \\ x_3 \end{bmatrix} + B \begin{bmatrix} \tau_x \\ \tau_y \\ \tau_r \end{bmatrix}$$
$$\begin{bmatrix} u \\ v \\ r \end{bmatrix} = C \begin{bmatrix} x_1 \\ x_2 \\ x_3 \end{bmatrix} + D \begin{bmatrix} \tau_x \\ \tau_y \\ \tau_r \end{bmatrix} \tag{2}$$

Matrix **A**, **B** and **C** of the controlled object, which is the *Blue Lady* training ship model, are as shown below:

$$\mathbf{A} = \begin{bmatrix} -3.36 \cdot 10^{-5} & 0 & 0 \\ 0 & -9.0 \cdot 10^{-3} & -2.0 \cdot 10^{-4} \\ -3.0 \cdot 10^{-3} & -1.0 \cdot 10^{-2} & -7.7 \cdot 10^{-3} \end{bmatrix} \tag{3}$$

$$\mathbf{B} = \begin{bmatrix} 3.62 \cdot 10^{-3} & 0 & 0 \\ 0 & 2.06 \cdot 10^{-3} & -1.3 \cdot 10^{-5} \\ 3.0 \cdot 10^{-5} & 1.15 \cdot 10^{-5} & 8.0 \cdot 10^{-3} \end{bmatrix} \tag{4}$$

$$\mathbf{C} = \begin{bmatrix} 1 & 0 & 0 \\ 0 & 1 & 0 \\ 0 & 0 & 1 \end{bmatrix} \tag{5}$$

$$\mathbf{D} = \begin{bmatrix} 0 & 0 & 0 \\ 0 & 0 & 0 \\ 0 & 0 & 0 \end{bmatrix} \tag{6}$$

3. State space control

During controller synthesis for the controlled object defined with matrices a state space controller K was received, in which output signal z for specific given values u, v, r had a control error e_{stat} . Figure 3(a) shows a simplified block diagram of the control system with an integrating element.

Achieving a static accuracy where control error reaches zero is possible by using an ideal integrating element with a transfer function of:

$$G_i(s) = \frac{k_i}{s} \tag{7}$$

where k_i is the gain of the integrating element (equal = 1). While examining a multidimensional controlled object it was observed that adding an ideal integrating element does not provide expected results. One of the disadvantages of a control system is the fact that gain can change in a closed loop system when controlled object parameters change. To avoid adjusting gain every time a given value parameter changes, which is common in this system, an additional closed loop with an inertial element was added. This allows to a steady closed loop system static accuracy despite given value parameter changes. However, implementing and integrating element worsens stability of the whole control system. As a result of an LMI controller synthesis for a given value of longitudinal velocity $u = 0.1$ m/s where velocities equal to $v = 0$ m/s and rotational $r = 0$ rad/s , which in Figure 4 is the dashed line. Controlled velocity is marked in Figure 4 with the solid line. Figure 4 shows clearly that using an integrating element significantly worsens the stability of a multidimensional control system. It influences system dynamics and does not fulfil control criteria.

A solution which eliminates the above relation but still keeps control error at zero ($s = 0$) is replacing the integrating element with a first stage inertial element with a very high gain, its transfer function as shown below:

$$T(s) = \frac{k_{in}}{T_{in}s + 1} \tag{8}$$

where k_{in} is gain and T_{in} is the time constant. Similar assumptions have been made by authors of [24,25]. Step response of a first stage inertial element is shown in Figure 5, the first part of the graph is highlighted to point out how similar it is to an ideal integrating element.

This method allows bringing control error down to zero with a first stage inertial element when correct values of k_{in} and T_{in} are selected, not equal zero. Controlled object parameters change depending on many factors like cargo weight or ship's speed. As shown in [26] to avoid adjusting static gain every time controlled

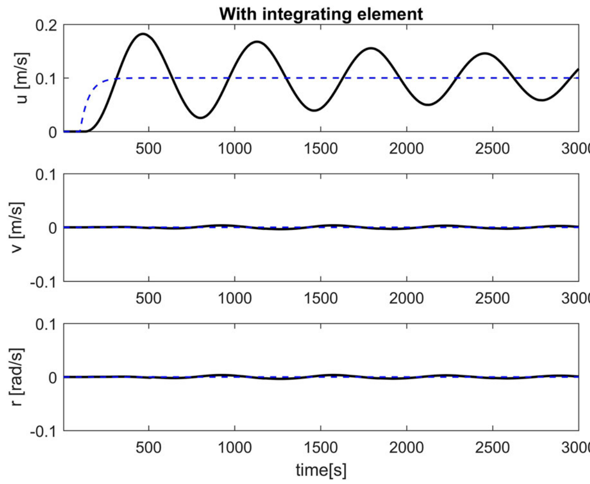

Figure 4. Ahead manoeuver with longitudinal velocity $u = 0.1$ m/s, lateral $v = 0$ m/s and rotational $r = 0$ rad/s velocities with manoeuver duration of 3000 s with integrating element included in the control system. Dashed line – given value and solid line – controlled value.

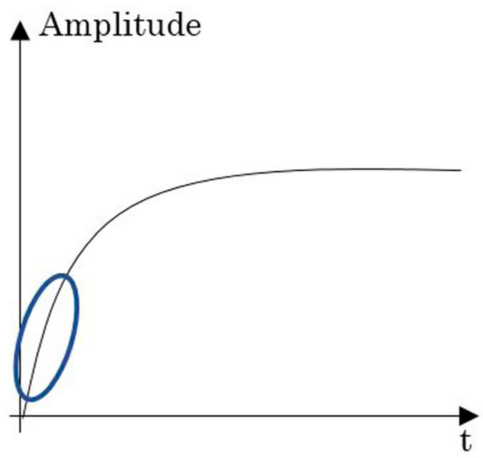

Figure 5. Step response of a first stage inertial element.

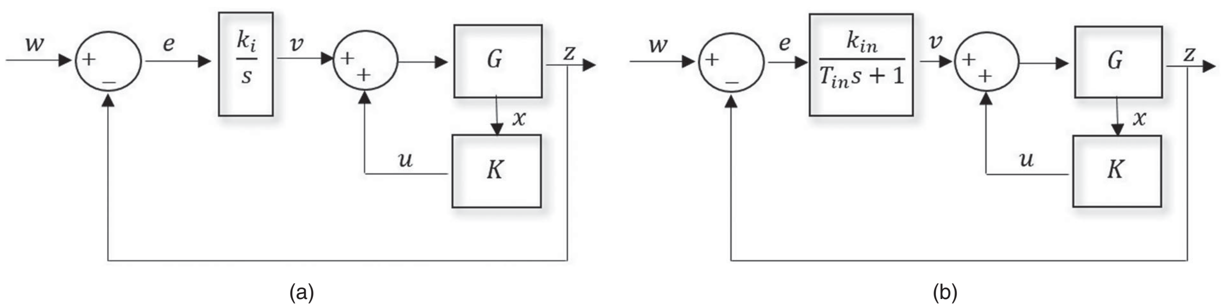

Figure 3. Simplified block diagram of the control system with elements. (a) With an integrating element. (b) With a first stage inertial element.

object parameters change a different control system structure was used, as shown in Figure 3(b), where state space equations are as follows:

$$\begin{aligned} \dot{x}(t) &= (\mathbf{A} + \mathbf{B}_u K)x(t) + \mathbf{B}_w w(t) \\ z(t) &= (\mathbf{C} + \mathbf{D}_u K)x(t) + \mathbf{D}_w w(t) \end{aligned} \tag{9}$$

State space equations of the first stage inertial element from Figure 3(a) block diagram are as shown below:

$$\begin{aligned} \dot{x}_{in} &= \mathbf{A}_{in} x_{in} + \mathbf{B}_{in} e \\ v &= \mathbf{C}_{in} x_{in} + \mathbf{D}_{in} e \end{aligned} \tag{10}$$

Values of k_{in} and T_{in} were selected by experimenting and for these values the inertial element matrices have the form of:

$$\mathbf{A}_{in} = \begin{bmatrix} -0.25 \cdot 10^{-4} & 0 & 0 \\ 0 & -0.25 \cdot 10^{-4} & 0 \\ 0 & 0 & -0.25 \cdot 10^{-4} \end{bmatrix} \tag{11}$$

$$\mathbf{B}_{in} = \begin{bmatrix} 0.25 & 0 & 0 \\ 0 & 0.25 & 0 \\ 0 & 0 & 0.25 \end{bmatrix} \tag{12}$$

$$\mathbf{C}_{in} = \begin{bmatrix} 0.3 & 0 & 0 \\ 0 & 0.3 & 0 \\ 0 & 0 & 0.3 \end{bmatrix} \tag{13}$$

$$\mathbf{D}_{in} = \begin{bmatrix} 0 & 0 & 0 \\ 0 & 0 & 0 \\ 0 & 0 & 0 \end{bmatrix} \tag{14}$$

Block diagram from Figure 6 shows connections between the controlled object, *Blue Lady* ship model, first stage inertial element and state space controller, described as LMI gain controller. The method described in this paper required to incorporate an inertial element matrix into a multidimensional controlled object matrix. State space equations of the closed loop control system with a multidimensional controlled object with an inertial element are shown below:

$$\underbrace{\begin{bmatrix} \dot{x}_{in} \\ \dot{x} \end{bmatrix}}_{\dot{x}} = \underbrace{\begin{bmatrix} \mathbf{A}_{in} - \mathbf{B}_{in}\mathbf{D}\mathbf{C}_{in} & -\mathbf{B}_{in}\mathbf{C} \\ \mathbf{B}\mathbf{C}_{in} & \mathbf{A} \end{bmatrix}}_{\mathbf{A}} \cdot \underbrace{\begin{bmatrix} x_{in} \\ x \end{bmatrix}}_{x} + \underbrace{\begin{bmatrix} \mathbf{B}_{in}\mathbf{D} \\ \mathbf{B} \end{bmatrix}}_{\mathbf{B}_u} \cdot u + \underbrace{\begin{bmatrix} \mathbf{B}_{in} \\ 0_{[3x3]} \end{bmatrix}}_{\mathbf{B}_w} \cdot w$$

$$z = \underbrace{[\mathbf{D}\mathbf{C}_{in} \quad \mathbf{C}]}_{\mathbf{C}} \cdot \underbrace{\begin{bmatrix} x_{in} \\ x \end{bmatrix}}_{x} + \underbrace{[\mathbf{D}]}_{\mathbf{D}_u} u + \underbrace{[0_{[3x3]}]}_{\mathbf{D}_w} \cdot w \tag{15}$$

4. Linear matrix inequalities

LMI are a tool for convex optimization used among others for robust controller synthesis [13]. According to Laypunov the necessary and sufficient condition for a linear system to be asymptotically stable is finding a symmetrical and positively defined matrix $\mathbf{P} = \mathbf{P}^{\mathrm{T}}$, $\mathbf{P} \succ 0$[1] ($\mathbf{P}$ is the unknown variable), which after taking into consideration Schur's stability condition has the from of:

$$\begin{bmatrix} -\mathbf{A}^{\mathrm{T}}\mathbf{P} - \mathbf{P}\mathbf{A} & 0 \\ 0 & \mathbf{P} \end{bmatrix} \succ 0 \tag{16}$$

where matrix $\mathbf{A}$ is the controlled object and matrix $\mathbf{P}$ is the unknown.

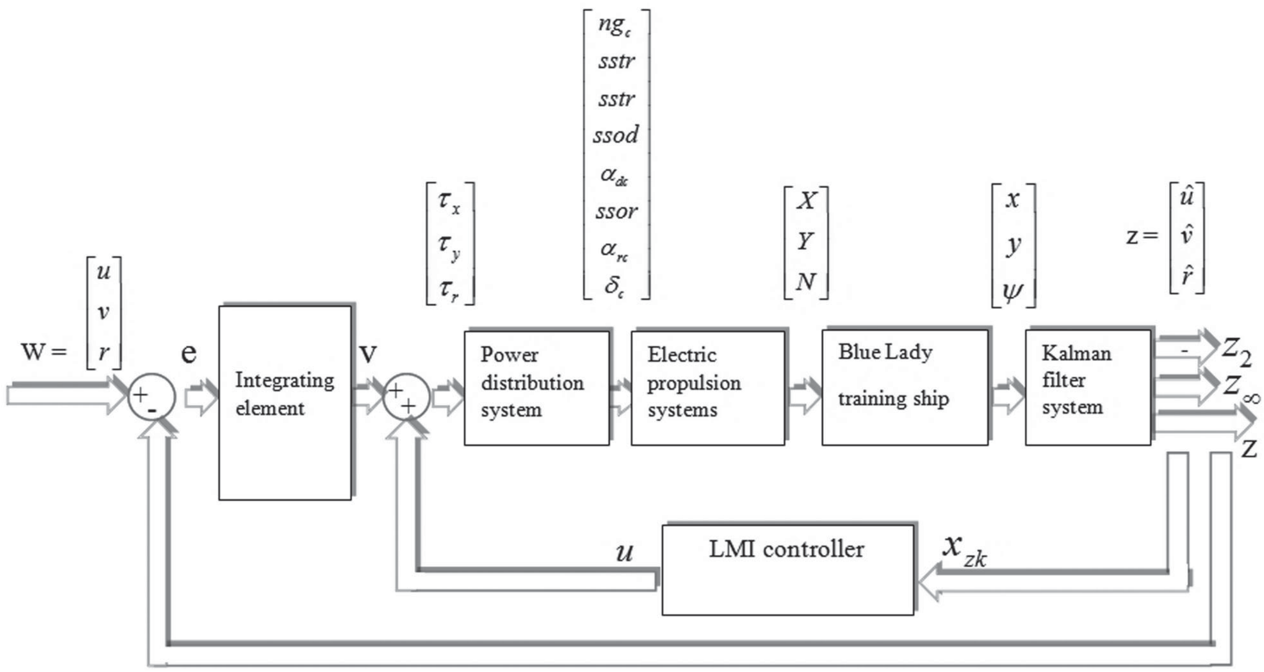

Figure 6. Block diagram of a closed loop, multidimensional control system with a state space controller, inertial element and a multidimensional controlled object with special signals described in Figure 2.

Due to the complexity of LMI as a whole, this paper will present only the stages necessary for adding a first stage inertial element to state space controller synthesis for improving system stability. Following controller synthesis was adopted for the multidimensional object of *Blue Lady* ship model.

The controller synthesis method for a state space regulator for a above ship model is shown in [27]. Based on simulation results controller structure based on a state space controller was chosen, where

$$u = \mathbf{K} \cdot x_{zk} \tag{17}$$

Specific stages of controller synthesis with a first stage inertial element will be described briefly below based on state space Equation (15). The first stage is to define the pole placement region located in the left half-plane of complex variable plane s in order to specify dynamic parameters of the designed closed loop system. First LMI condition:

$$\begin{aligned} \mathbf{R}_{\mathbb{D}}(\mathbf{A}, \mathbf{P}_{\text{reg}}) &= \mathbf{L} \otimes \mathbf{P}_{\text{reg}} + \mathbf{M} \otimes (\mathbf{A}\mathbf{P}_{\text{reg}}) \\ &+ \mathbf{M}^{\mathrm{T}} \otimes (\mathbf{A}\mathbf{P}_{\text{reg}})^{\mathrm{T}} \prec 0 \end{aligned} \tag{18}$$

is fulfilled if and only if there exists a symmetrical positively defined matrix $\mathbf{P}_{\text{reg}}$ where:

- $\mathbf{A}$ - however in this specific case instead of $\mathbf{A}$ matrix we have to use the form $= (\mathbf{A} + \mathbf{B}_u\mathbf{K})$,
- $\mathbf{P}_{\text{reg}}$ - the unknown, symmetrical positively defined Laypunov matrix $\mathbf{P} \succ 0, \mathbf{P} = \mathbf{P}^{\mathrm{T}}$,
- $\mathbf{L}, \mathbf{M}$ - specific, user defined matrices, where pole placement area is selected based on closed loop system dynamics.

The second stage is H_∞ minimization related with an estimation of scalar value γ_∞ which is the upper limit of the H_∞ standard. When determining the smallest value of γ_∞ for the given pole placement region, of the closed loop system, we assume that the obtained scalar value γ_∞ is constant. Scalar value γ_∞ can be calculated based on H_∞ minimization or it can be assumed to be a constant limit. Second LMI condition:

$$\begin{bmatrix} \mathbf{A}\mathbf{P}_\infty + \mathbf{P}_\infty\mathbf{A}^{\mathrm{T}} & \mathbf{B}_w & \mathbf{P}\mathbf{C}^{\mathrm{T}} \\ \mathbf{B}_w{}^{rmT} & -\gamma_\infty^2\mathbf{I} & \mathbf{D}^{\mathrm{T}} \\ \mathbf{C}\mathbf{P} & \mathbf{D} & -\mathbf{I} \end{bmatrix} \prec 0 \tag{19}$$

The above equation is generic and in this specific case, taking into account Equation (15), it has the below form:

- $\mathbf{A} = (\mathbf{A} + \mathbf{B}_u\mathbf{K})$.

The third stage is H_2 standard minimization. One of the ways of obtaining that is looking for γ_2 for the value obtained in the second stage above:

$$\gamma_\infty > \gamma_{\infty\min} \tag{20}$$

The third LMI condition:

$$\begin{gathered} \begin{bmatrix} \mathbf{A}\mathbf{P}_2 + \mathbf{P}_2\mathbf{A}^{\mathrm{T}} & \mathbf{B}_w \\ \mathbf{B}_w{}^{\mathrm{T}} & -\mathbf{I} \end{bmatrix} \prec 0 \\ \begin{bmatrix} \mathbf{Q} & \mathbf{C}^{\mathrm{T}} \\ \mathbf{C} & \mathbf{P}_2 \end{bmatrix} \succ 0 \\ Tr(\mathbf{Q}) < \gamma_2^2 \end{gathered} \tag{21}$$

This means that LMI conditions formulated for H_∞ by Equation (19), for H_2 by Equation (21) and for chosen pole placement (Equation (18)) are fulfilled if there exists a symmetrical positively determined Laypunov matrix. The final form of state space controller gain matrix $\mathbf{K}$, that stabilizes the whole control system and minimizes H_∞ and H_2 standards. Because matrix $\mathbf{P}$ is positively determined there exists its converse matrix $\mathbf{Y}$ and so space state controller matrix $\mathbf{K}$ can be described as

$$\mathbf{K} = \mathbf{Y}\mathbf{X}^{-1} \tag{22}$$

Multitasking of LMI used for space state controller synthesis, for a multidimensional object, means that several design criteria are met at the same time, as explained in [9,13]. In this paper, the closed loop system state space controller was determined by three main stages as detailed in [27]. Based on the first stage inertial element implementation values of state space matrix $\mathbf{K}$ are

$$\mathbf{K} = \begin{bmatrix} 1498.854 & 0.048 & 0.265 & -799.670 & -0.016 & -0.158 \\ -0.0306 & 1696.219 & -5.115 & 0.0151 & -952.017 & 3.259 \\ -5.683 & -1.625 & 440.994 & 3.443 & 1.026 & -247.154 \end{bmatrix}$$

5. Model validation

Matlab software package includes several libraries useful for calculations using LMI in automation, for example:

- YALMIP (Yet Another LMI Preprocessor) and SeDuMi (Self – Dual – Minimization);
- YALMIP and SDPT3 (semidefinite-quadratic-linear programming) [28];
- CVX (Disciplined Convex Programming) [29].

Two among them, Yalmip and SeDuMi, are especially useful in calculations using LMIs. Both of them are based on a “public domain” license and can be freely downloaded from:

- http://sedumi.ie.lehigh.edu/ [30],
- http://users.isy.liu.se/johanl/yalmip/ [31].

Table 1. Comparison of mean deviation from given values described in (23).

Mnvr.	Signal	Without inertial element	With inertial element
1	$\Delta u(\%)$	0.078	0.0001
2	$\Delta u(\%)$	0.145	0.0001
	$\Delta v(\%)$	0.028	0.0002
3	$\Delta u(\%)$	0.072	0.0003
	$\Delta v(\%)$	0.007	0.0006
	$\Delta r(\%)$	0.193	0.0015

For the above case study, computer simulations were performed using Matlab software with YALMIP and SeDuMi. Table 1 shows a comparison of mean values for deviations from given values. In order to determine the quality of control the following formula was used:

$$\Delta x\% = \frac{\sqrt{\sum_{n}^{1}(x_{\text{given}} - x_{\text{control}})^2}}{n} \cdot 100 \tag{23}$$

where n is the number of measurements; x is the deviation value, in percentage, of measured parameter $x \in u, v, r$; x_{given} is the reference signal value (given value) and x_{control} is the output signal value received from the system.

Computer simulations were made for the below three types of ship movement:

- **Manoeuver 1** Ahead movement with a given longitudinal velocity $u = 0.1$ m/s, with manoeuver duration of 3000 s. Given values of lateral and rotational velocities were set to $v = 0$ m/s, $r = 0$ deq/s. This type of ship maoneuver, at low velocities, is very common when navigating narrow passages like channels, rivers or entering harbours. Simulation results with the use of an integrating element are shown in Figure 7(a) while simulation results with the first stage inertial element are presented in Figure 7(b).

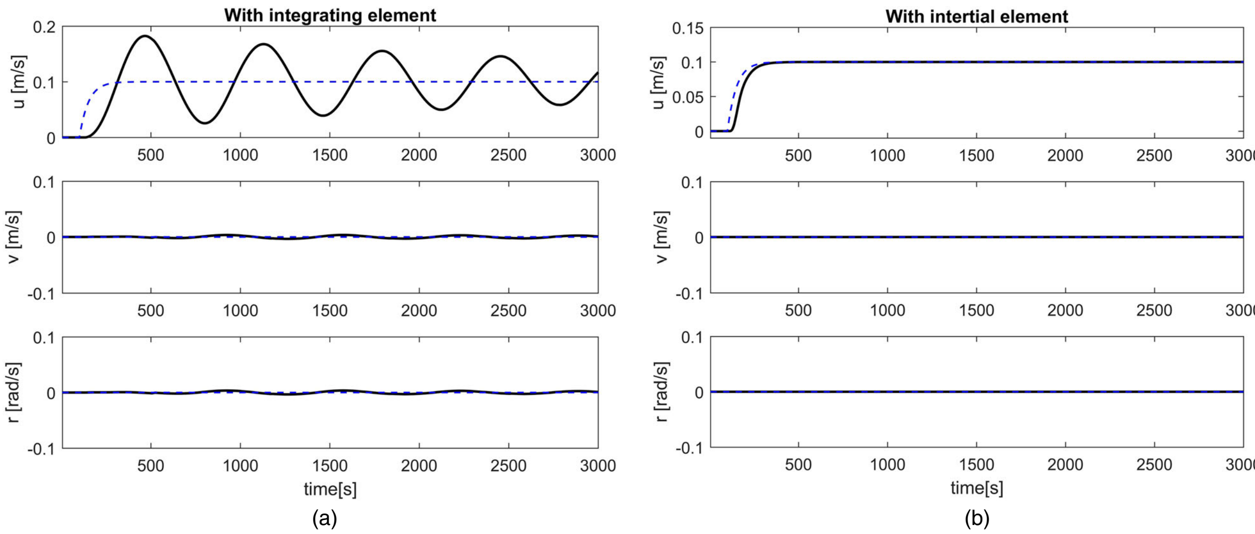

Figure 7. Ahead manoeuver with longitudinal velocity $u = 0.1$ m/s, $v = 0$ m/s, $r = 0$ rad/s and manoeuver duration 3000 s. Dashed line – given value and solid line – controlled value. (a) With the use of an integrating element. (b) With the use of an inertial element.

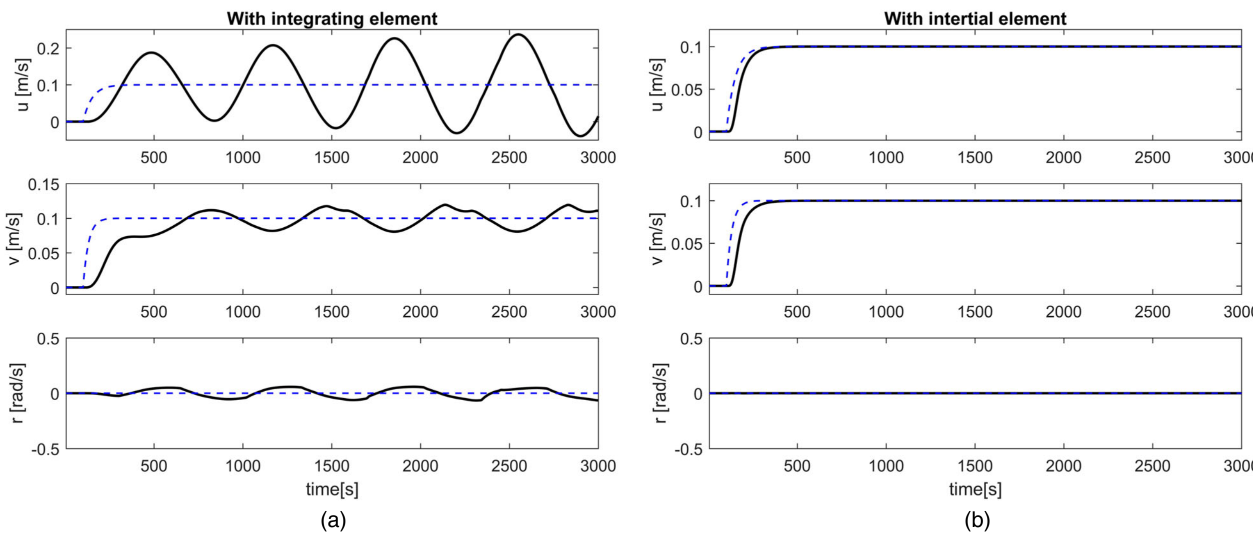

Figure 8. Ahead manoeuver with longitudinal velocity $u = 0.1$ m/s, $v = 0.05$ m/s, $r = 0$ rad/s and manoeuver duration 3000 s. Dashed line – given value and solid line – controlled value. (a) With the use of an integrating element. (b) With the use of an inertial element.

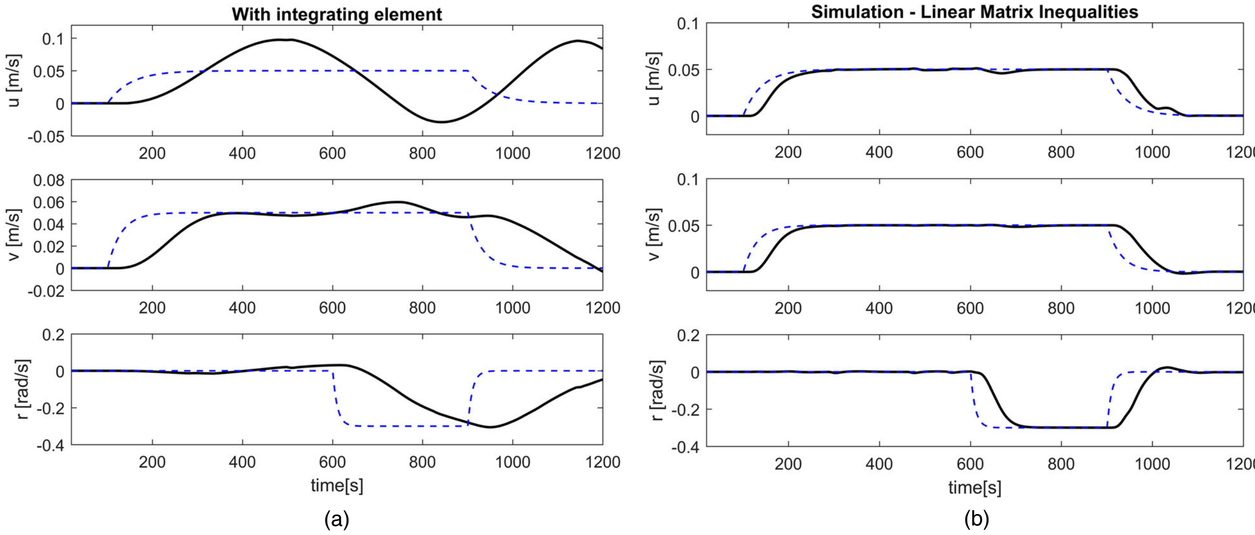

Figure 9. Ahead manoeuver with longitudinal velocity $u = 0.1$ m/s, $v = 0.05$ m/s, $r = -0.3$ rad/s and manoeuver duration 1200 s. Dashed line – given value and solid line – controlled value. (a) With the use of an integrating element. (b) With the use of an inertial element.

- **Manoeuver 2** Ahead and sideways movement with given longitudinal $u = 0.1$ m/s and lateral $v = 0.05$ m/s velocities and rotational velocity equal to $r = 0$ deq/s velocities with manoeuver duration of 3000 s. This type of ship manoeuver, at low velocities, is a typical approach to berth which is located parallel to ships course. Simulation results with the use of an integrating element are shown in Figure 8(a) while simulation results with the first stage inertial element are presented in Figure 8(b).

- **Manoeuver 3** Ahead and sideways movement with rotation, with given longitudinal $u = 0.1$ m/s, lateral $v = 0.05$ m/s and rotational $r = 0.03$ deq/s velocities with manoeuver duration of 1200 s. This type of ship manoeuver, at low velocities, is a typical approach to berth which is located perpendicular to ships course. Simulation results without the use of an inertial element are shown in Figure 9(a) while simulation results with the first stage inertial element are presented in Figure 9(b).

The proposed method proves to be a good tool for lowering control error down to zero in state space controller synthesis for a multidimensional controlled object. Computer simulations show that a first stage inertial element gives the benefits of an ideal integrating element without its negative influence on system stability.

6. Conclusions

This paper presented the benefits of implementing a first stage inertial element to a closed loop control system with a state space controller using LMI. Inertial element implementation steps were shown, followed by computer simulation results for precision ship movement control of *Blue Lady* VLCC ship model. The proposed method proves to be a good tool for lowering control error down to zero in state space controller synthesis for a multidimensional controlled object. Conducted computer simulations prove the validity of using a first stage inertial element. As an example deviations of controlled values from given values for longitudinal velocity $u = 0.1$ m/s and lateral velocity $v = 0.1$ m/s, while using a first stage inertial element, are several orders of magnitude lower than while using an ideal integrating element. Additionally using the inertial element doesnot have the negative impact on system stability as the integrating element does. Control error in computer simulations without the inertial element was out of range. While after including the inertial element it was within the range of 0.0001% to 0.0015%. Reducing control error had a direct impact on ship movement control precision. Thanks to the possibility of cooperation with the Foundation for Safety of Navigation and Environment Protection future will studies should include testing the validity of using a first stage inertial element in real life Silm Lake trials in Ilawa [32]. First stage of real life testing will be done on open water due to the safety of the *Blue Lady* ship model and its operators. If results of the first stage will prove to be satisfactory, the testing will be done while actually navigating narrow passages and berthing both parallel and perpendicular to ships course. The Silm Lake training centre has the infrastructure to train various types of ship manoeuvers including narrow passages and various harbour and berth configurations.

Note

1. The problem of finding a symmetrical, positively defined matrix **P** is often called the *feasibility problem*.

Disclosure statement

No potential conflict of interest was reported by the author.

References

[1] Lazarowska A. A new deterministic approach in a decision support system for ships trajectory planning. Expert Syst Appl. 2017;71:469–478.
[2] Mohamed-Seghir M. Computational intelligence method for ship trajectory planning. 2016 21st International Conference on Methods and Models in Automation and Robotics (MMAR); 2016 Aug; Miedzyzdroje, Poland. p. 636–640.
[3] Lisowski J. Analysis of methods of determining the safe ship trajectory. TransNav. 2016;10(2):223–228.
[4] Kula KS. Model-based controller for ship track-keeping using neural network. 2015 IEEE 2nd International Conference on Cybernetics (CYBCONF); 2015 Jun; Gdynia, Poland. p. 178–183.
[5] Lebkowski A. Evolutionary methods in the management of vessel traffic. In: Weintritt, Neumann T, editors. Information, communication and environment. London: CRS Press/Balkema; 2015. p. 259–266.
[6] Benlahrache MA, Othman S, Sheibat-Othman N, Multivariable model predictive control of wind turbines in presence of actuator fault. 2017 8th International Renewable Energy Congress (IREC); 2017 Mar; Amman, Jordan. p. 1–6.
[7] Tomera M. A multivariable low speed controller for a ship autopilot with experimental results. 2015 20th International Conference on Methods and Models in Automation and Robotics (MMAR); 2015 Aug; Miedzyzdroje, Poland. p. 17–22.
[8] Gierusz W. The h_2 and robust h_∞ regulators applied to multivariable ship steering. TransNav. 2009;3(4): 431–440.
[9] Boyd S, Ghaoui EL, Feron E, et al. Linear matrix inequalities in system and control theory. Philadelphia (PA): SIAM; 1994.
[10] Ostertag E. Mono-and multivariable control and estimation: linear, quadratic and LMI methods. Berlin: Springer-Verlag; 2011.
[11] Lam H, Leung F. Stability analysis of fuzzy-model-based control systems. Berlin: Springer-Verlag; 2011.
[12] Ebihara Y, Peaucelle D, Arzelier D. S-variable approach to LMI-based robust control. London: Springer-Verlag; 2015.
[13] Duan GR, Yu HH. LMIs in control systems: analysis, design and applications. Boca Raton (FL): CRC Press; 2013.
[14] Rogers E, Galkowski K, Paszke W, et al. Multidimensional control systems: case studies in design and evaluation. Multidimens Syst Signal Process. 2015;26(4): 895–939.
[15] Joelianto E, Gani G, Putri NK, et al. Robust control with linear matrix inequality approach for ship steering problem. 2016 International Conference on Instrumentation, Control and Automation (ICA); Bandung, Indonesia. IEEE; 2016. p. 126–131.
[16] Peng Y, Zhu Q, Nouri H. Mixed H2/Hinf robust controller design based LMI techniques. Berlin: Springer; 2014. p. 325–369.
[17] Chairinnas Joelianto E, Gani G, et al. Robust control with linear matrix inequality approach for ship steering problem. 2016 International Conference on Instrumentation, Control and Automation (ICA); 2016 Aug; Bandung, Indonesia. p. 126–131.
[18] Iqbal S, Bhatti AI. Load varying polytopic based robust controller design in LMI framework for a 2DOF stabilized platform. Arabian J Sci Eng. 2011;36(2):311–327.
[19] Gierusz W. Simulation model of the shiphandling training boat "blue lady". Proceedings of Control Applications in Marine Systems, Glasgow, UK; 2001.
[20] Gierusz W, Tomera M. Logic thrust allocation applied to multivariable control of the training ship. Control Eng Pract. 2006;14(5):511–524.
[21] Gierusz W, Rak A, Pomirski J. Control system for trials on material ship model. Pol Marit Res. 2012;S1: 25–30.
[22] Rybczak M. Linear matrix inequalities in multivariable ship's steering. Pol Marit Res. 2012;S1:37–44.
[23] Miller A. Identification of a multivariable incremental model of the vessel. 2016 21st International Conference on Methods and Models in Automation and Robotics (MMAR); 2016 Aug; Miedzyzdroje, Poland. p. 218–224.
[24] Di Ruscio D. Model predictive control with integral action: a simple MPC algorithm. Model Ident Control. 2013;34(3):119–129.
[25] Alepuz S, Salaet J, Gilabert A, et al. Optimal regulator with integral action and gain-scheduling for the comprehensive control of three-level NPC VSI. 2003 IEEE 34th Annual Power Electronics Specialist Conference. PESC '03; Vol. 3; 2003 Jun; Acapulco, Mexico. p. 1420–1425.
[26] Kaczorek TWektory i macierze w automatyce i elektrotechnice. Wydawnictwo Naukowo-Techniczne (WNT); 1998; Poland.
[27] Miller A, Rybczak M. Methods of controller synthesis using linear matrix inequalities and model predictive control. Sci J Marit Unive Szczecin. 2015;43(115): 22–28.
[28] Toh K-C, Todd M, Tutuncu RH. On the implementation and usage of SDPT3 – a MATLAB software package for semidefinite-quadratic-linear programming. Version 4.0. 2010.
[29] Gustafsson M, Tayli D, Ehrenborg C, et al. Antenna current optimization using MATLAB and CVX. FERMAT. 2016;15.
[30] Sturm J. Using SeDuMi 1.02, a MATLAB* toolbox for optimization over symmetric conest; 2001. Available from: http;//fewcal.kub.nl/sturm.
[31] Löfberg J. YALMIP: a toolbox for modeling and optimization in MATLAB. 2004 IEEE International Symposium on Computer Aided Control Systems Design. IEEE; 2004. p. 284–289.
[32] Ilawa. Foundation for safety of navigation and environment protection; 2017. Available from: https://www.ilawashiphandling.com.pl/about.html.